AIAA JOURNAL
Vol. 37, No. 11, November 1999

Theory of Flame Histories in Droplet Combustion at Small Stoichiometric Fuel–Air Ratios

F. F. Fachini*
National Space Research Institute, 12630-000 São Paulo, Brazil
A. Liñán†
Universidad Politénica de Madrid, 28040 Madrid, Spain
and
F. A. Williams‡
University of California, San Diego, La Jolla, California 92093-0411

Motivated by observations on the spherically symmetrical burning of single, free heptane droplets in quiescent helium–oxygen atmospheres, made in Spacelab aboard the Space Shuttle, the theory of droplet burning is extended for conditions under which the Burke–Schumann flame sheet lies in the outer transient zone. Account is taken of Lewis numbers different from unity and of radiant energy loss that sometimes leads to extinction. The asymptotic analysis employs the square root of the ratio of the gas to liquid density as a small parameter. In suitably scaled outer variables, the droplet then appears as a time-varying point source, and the flame radius first grows then decreases in size. Numerical integrations of the outer parabolic partial differential equations provide flame histories and histories of the outer temperature and concentration fields. An analytical criterion for flame extinction enables the extinction point along the flame history to be determined, when extinction is caused by radiative energy loss. The theoretical results can be useful for comparison with experiment and for predicting whether radiative extinction will occur in droplet combustion.

Introduction

COMBUSTION of an isolated droplet is a classical problem about which a great deal of research has been performed.[1] Practical motivations for such studies range from interest in improving the cleanliness and efficiency of power production in liquid-fueled combustion chambers to concerns about fire safety. Despite the large amount of work that has been devoted to the subject, there remain outstanding questions in need of fundamental clarification. The present contribution addresses some such questions related to time-dependent behavior and flame extinction.

Because droplet combustion generally is diffusion controlled, the burning time of a droplet is approximately proportional to the square of its initial diameter. This result can be obtained by dimensional analysis because the ratio of the diameter squared to the burning time has units of a diffusion coefficient, the physical property controlling the burning rate. The classical theory addresses representative conditions under which, moreover, the ratio ε of the gas density to the liquid density is a small parameter, so that quasisteady behavior prevails near the droplet, and the square of the droplet diameter decreases approximately linearly with time. Far from the droplet, however, conditions remain transient because the time for information about the initial condition to propagate diffusively outward again is proportional to the square of the initial diameter, from dimensional considerations. Theories have been developed in which solutions in the inner quasisteady and outer transient zones are matched through an asymptotic expansion in the small parameter ε (Refs. 2 and 3). The present work extends this type of theory, focused on the outer transient zone.

The conditions addressed are those under which the flame lies in the outer transient zone. These conditions prevail for sufficiently large values of the stoichiometric air–fuel ratio $s = \nu/Y_{O\infty}$, where ν is the mass of oxidizer required to burn a unit mass of fuel and $Y_{O\infty}$ is the mass fraction of oxidizer in the ambient atmosphere. Here s may be interpreted as the mass of the atmospheric gas required to burn a unit mass of fuel; the flame is in the outer zone if s is of the order of $\varepsilon^{-1/2}$ or larger. Indeed, typical values of s and $\varepsilon^{-1/2}$ are 20 and 30, respectively, for liquid hydrocarbon droplets burning in air at normal atmospheric pressure. The value of s was varied systematically in recent Spacelab experiments[4] by changing $Y_{O\infty}$, assuring that in some of the tests, those in the dilute atmospheres, the flame lies in the outer transient zone. An objective of the present theory is to develop results that can be compared quantitatively with these Spacelab measurements.

The present theory differs from earlier asymptotic theories of this type by building on recent results[5] to account for Lewis numbers of the fuel and oxidizer that are different from unity. Because Lewis numbers are appreciably greater than unity in the Spacelab experiments,[4] this extension is necessary in seeking quantitative comparisons. Such extensions have been employed recently in related analysis of different problems.[6,7]

The experiments[4] often revealed radiative extinction of the flame after its diameter had grown sufficiently large. In these radiative extinctions, energy losses by radiant emissions from CO_2 and H_2O bands extinguish the flame well before the droplet disappears. To account for this effect, radiant energy loss is included in the present analysis. A flame-extinction criterion based on activation-energy asymptotics[8] is applied to determine when the flame will extinguish. Because the flame is in the outer zone, the temperature is nearly constant on the fuel side of the flame, and therefore, it is necessary to account for the radiant loss throughout this fuel region of the transient zone, rather than employing asymptotics[9] based on a strong temperature sensitivity of the radiant loss rate. The previous radiant-loss analyses[10] are, thus, more appropriate for conditions under which the flame is in the quasisteady region, a condition not addressed here.

Received 9 September 1998; presented as Paper 99-0586 at the 37th Aerospace Sciences Meeting, Reno, NV, 11–14 January 1999; revision received 12 February 1999; accepted for publication 23 March 1999.

*Researcher, Laboratório de Combustão e Propulsão, Caxia Postal 01, Rodovia Presidente Dutra Km 40, Cachoeira Paulista; also Visiting Scholar, Center for Energy and Combustion Research, Department of Applied Mechanics Engineering Science, University of California, San Diego, La Jolla, CA 92093-0411; fachini@yabae.cptec.inpe.br.

†Professor of Fluid Mechanics, Escuela Superior de Ingenieros Aeronáuticos, Plaza Cardenal Cisneros 3; also Visiting Professor, Center for Energy and Combustion Research, Department of Applied Mechanics Engineering Science, University of California, San Diego, La Jolla, CA 92093-0411.

‡Professor of Engineering Physics and Combustion, Center for Energy and Combustion Research, Department of Applied Mechanics Engineering Science, 9500 Gilman Drive. Fellow AIAA.

An alternative to beginning with an expansion in ε is a direct numerical onslaught on the original spherically symmetrical, time-dependent partial differential equations. Such attacks have been mounted in the past and applied to heptane,[11] benzene,[12] and methanol[13] droplet combustion, each with differing radiative-transfer approximations. Despite uncertainties in chemical kinetics and molecular transport properties, these full numerical integrations have produced interesting results, although additional parameters appear that need to be assigned values. The present approach serves to remove, for example, the ratio of the gas to liquid density as a parameter whose value must be selected to proceed, and it thereby provides explicit functional dependences and scalings that can be extracted from fully numerical solutions only through excessive labor.

Mathematical Formulation

In addition to the nondimensional parameters $\varepsilon \ll 1$ and $s \gg 1$, relevant parameters are the nondimensional heat release $q = Q_F/(c_p T_\infty)$, the constant fuel and oxidizer Lewis numbers, $Le_F = \alpha_\infty/D_{F\infty}$ and $Le_O = \alpha_\infty/D_{O\infty}$, and the normalized emissivity

$$\sigma = \frac{4a_0^2\sigma_B T_\infty^3(\theta_{af}^4 - 1)}{l_{P af}c_p\rho_\infty\alpha_\infty\varepsilon} \tag{1}$$

along with appropriate chemical-kinetics parameters. Q_F is the energy released per unit mass of fuel consumed, c_p is the specific heat at constant pressure for the mixture, assumed constant, T is temperature, the subscript ∞ identifies conditions in the ambient atmosphere, D_F and D_O are diffusion coefficients, the subscripts F and O identify fuel and oxidizer, α is the thermal diffusivity of the mixture, ρ is density, $l_{P af}$ is a representative constant value of the Planck-mean absorption length, and σ_B is the Stefan–Boltzmann constant. To be specific, $l_{P af}$ may be taken to be the value that would apply at a Burke–Schumann flame sheet if Lewis numbers were unity. The droplet radius, a function of time t, is denoted by $\bar{a}$, and its initial value is identified by the subscript 0, as are all initial conditions. The subscript af identifies the adiabatic flame temperature that would prevail at the Burke–Schumann flame sheet if all Lewis numbers were unity. Appropriate nondimensional variables are

$$\tau = (t\alpha_\infty/\bar{a}_0^2)(\rho_\infty/\rho_l), \qquad x = r/\bar{a}_0, \qquad a = \bar{a}/\bar{a}_0$$
$$v = V_G a_0/\alpha_\infty, \qquad \varrho = \rho/\rho_\infty$$
$$y_O = Y_O/Y_{O\infty}, \qquad \theta = T/T_\infty \tag{2}$$

where the subscript l denotes conditions in the liquid, r are the radial coordinates, V_G is the gas velocity, and Y_i is the mass fraction of species i.

The gas-phase equations for conservation of mass, fuel, oxidizer, and energy can be written, respectively, in nondimensional form as

$$\varepsilon\frac{\partial\varrho}{\partial\tau} + \frac{1}{x^2}\frac{\partial}{\partial x}(x^2\varrho v) = 0 \tag{3}$$

$$\varepsilon\varrho\frac{\partial Y_F}{\partial\tau} + \varrho v\frac{\partial Y_F}{\partial x} = \frac{1}{x^2}\frac{\partial}{\partial x}\left(x^2\frac{f}{Le_F}\frac{\partial Y_F}{\partial x}\right) - \dot{\omega} \tag{4}$$

$$\varepsilon\varrho\frac{\partial y_O}{\partial\tau} + \varrho v\frac{\partial y_O}{\partial x} = \frac{1}{x^2}\frac{\partial}{\partial x}\left(x^2\frac{f}{Le_O}\frac{\partial y_O}{\partial x}\right) - s\dot{\omega} \tag{5}$$

$$\varepsilon\varrho\frac{\partial\theta}{\partial\tau} + \varrho v\frac{\partial\theta}{\partial x} = \frac{1}{x^2}\frac{\partial}{\partial x}\left(x^2 f\frac{\partial\theta}{\partial x}\right) + q\dot{\omega} - \varepsilon\sigma g\frac{\theta^4 - 1}{\theta_{af}^4 - 1} \tag{6}$$

where the function f accounts for the variation of the pressure-independent product $\rho\alpha = f\rho_\infty\alpha_\infty$, the function g accounts for the variation of the Planck-mean absorption length l_P according to $l_P = l_{P af}/g$, and the nondimensional reaction rate is $\dot{\omega} = \omega_F a_0^2/(\rho_\infty\alpha_\infty)$, where ω_F is the mass rate of consumption of the fuel per unit volume. Corresponding equations for conservation of product species, readily added, would be useful, for example, for evaluating variations of g, but for simplicity this is left for future work.

These equations involve a one-step approximation for the chemistry, the rate for which later is taken to be Arrhenius as a qualitatively reasonable approximation that can be related to elementary chemistry in future work. Soot formation is neglected, and the chemistry is assumed to be restricted to a narrow zone in the vicinity of the Burke–Schumann sheet that would occur in the limit of infinite reaction rate. Approximations of binary diffusion through an inert present in excess, with constant Lewis numbers and negligible Soret and Dufour effects, are introduced. The gas is assumed to be ideal with constant average molecular weight, and Mach numbers are low, giving $\varrho\theta = 1$ (constant pressure), and momentum conservation is superfluous. The radiation is treated in an optically thin, transparent-gas approximation, with the Planck-mean absorption length to be calculated from the known spectral bands of CO_2 and H_2O.

The boundary conditions for the gas-phase conservation equations are

$$\left(x^2 f\frac{\partial\theta}{\partial x}\right)_s + a^2 q' = \lambda l, \quad \text{at} \quad x = a \tag{7}$$

$$\lambda Y_{Fs} - \left(x^2\frac{f}{Le_F}\frac{\partial Y_F}{\partial x}\right)_s = \lambda, \quad \text{at} \quad x = a \tag{8}$$

$$\lambda y_{Os} - \left(x^2\frac{f}{Le_O}\frac{\partial y_O}{\partial x}\right)_s = 0, \quad \text{at} \quad x = a \tag{9}$$

and $\theta - 1 \to \varrho - 1 \to y_O - 1 \to Y_F \to 0$ as $x \to \infty$, where $\lambda = \dot{m}/(4\pi a_0\rho_\infty\alpha_\infty)$ and $l = L_V/(c_p T_\infty)$ are the nondimensional vaporization rate and the nondimensional heat of vaporization, respectively, in which vaporization Lewis number L_V is the heat of vaporization per unit mass of fuel, and the liquid is assumed to be at the boiling temperature T_l. The subscript s identifies conditions in the gas at the droplet surface. From overall energy conservation, $\theta_{af} = 1 + (q - l + \theta_l)/s$, which becomes $\theta_{af} = 1 + q/s$ when s and q are large, as considered later. Initial conditions exclude the droplet heating period and any excess fuel or energy deposited in the gas prior to ignition by the ignition mechanism.

The quantity q' is the nondimensional radiant energy flux at the droplet surface, the flux divided by $\rho_\infty\alpha_\infty c_p T_\infty/a_0$, assumed to be absorbed in a thin liquid layer at the droplet surface. The calculation of q' is a standard problem in radiative transfer and results, in a first approximation, in (Appendix A)

$$q' = \frac{\varepsilon\sigma}{2(\theta_{af}^4 - 1)}\int_{x_{min}}^{\infty} g(\theta^4 - 1)\,dx \approx \frac{\varepsilon\sigma x_f(\theta_f^4 - 1)}{2(\theta_{af}^4 - 1)} \tag{10}$$

when the flame is far from the droplet; here x_{min} is large compared with unity but small compared with the nondimensional flame radius x_f. The subscript f denotes condition at a Burke–Schumann flame sheet. In obtaining the approximate equality, variations of g are neglected, and the temperature is considered nearly constant in the outer zone inside the flame, with the variation of θ outside the flame occurring rapidly enough that the contribution from this zone can be neglected (a rough approximation).

Conservation of mass applied to the liquid phase leads to the expression

$$a^2 = 1 - 2\int_0^\tau\left(\frac{\lambda}{a}\right)d\tau \tag{11}$$

for the variation of the square of the droplet diameter. With the oxidizer Lewis number differing from unity, the ratio λ/a is no longer exactly constant[5] when the flame is far from the droplet, and q' can cause further departure from this classical diameter-squared law.

Solution in the Quasisteady Region

The nondimensional variables appearing in Eqs. (3–9) apply directly to the quasisteady region. The solution to leading order in ε can be obtained by omitting terms involving ε and reaction rates. It is, thereby, found from integrations that $x^2\varrho v = \lambda$ and

$$\left(\frac{y_O}{y_{Oa}}\right)^{1/Le_O} = (1 - Y_F)^{1/Le_F} = \frac{\theta + l - (a^2 q'/\lambda) - \theta_l}{\theta_a + l - (a^2 q'/\lambda) - \theta_l} \tag{12}$$

$$\frac{\lambda}{a}\left(1-\frac{a}{x}\right)=\int_{\theta_l}^{\theta}\frac{f(z)}{z+l-(a^2q'/\lambda)-\theta_l}\,\mathrm{d}z \tag{13}$$

where the subscript a identifies matching conditions with the outer-zone solutions for $x\to\infty$, the matching $Y_{Fa}=0$ has been anticipated, and the function f, accounting for variations of transport properties with θ, Y_F, and y_O, is expressed as a function of θ alone in Eq. (13) by use of the solutions in Eq. (12). The values of y_{Oa} and θ_a are to be determined by matching conditions, which will show that to leading order $y_{Oa}=0$ and, if the oxidizer Lewis number is unity and radiation is negligible, $\theta_a=\theta_f=\theta_{af}$. The burning-rate eigenvalue λ is determined in terms of θ_a by evaluating Eq. (13) at $x=\infty$, where $\theta=\theta_a$. From that evaluation it is seen that, if q' is negligible and θ_a is constant, λ/a is constant (the burning-rate or vaporization constant), giving the mass burning rate $\dot{m}$ proportional to $\bar{a}_0 a$ and resulting in the diameter-squared law from Eq. (11).

Description of the Transient Region

In the outer zone, the spatial variable of order unity is $X=\sqrt{(\varepsilon)}x$, and to leading order $Y_F=\sqrt{(\varepsilon)}y_F$, where y_F is of order unity. With these variables, Eqs. (3–6) become

$$\frac{\partial\varrho}{\partial\tau}+\frac{1}{X^2}\frac{\partial}{\partial X}(X^2\varrho V)=0 \tag{14}$$

$$\varrho\frac{\partial y_O}{\partial\tau}+\varrho V\frac{\partial y_O}{\partial X}=\frac{1}{X^2}\frac{\partial}{\partial X}\left(X^2\frac{f}{Le_O}\frac{\partial y_O}{\partial X}\right)-S\dot{\Omega} \tag{15}$$

$$\frac{\partial y_F}{\partial\tau}-\varrho V\frac{\partial y_F}{\partial X}=\frac{1}{X^2}\frac{\partial}{\partial X}\left(X^2\frac{f}{Le_F}\frac{\partial y_F}{\partial X}\right)-\dot{\Omega} \tag{16}$$

$$\frac{\partial\theta}{\partial\tau}-\varrho V\frac{\partial\theta}{\partial X}=\frac{1}{X^2}\frac{\partial}{\partial X}\left(X^2 f\frac{\partial\theta}{\partial X}\right)+Q\dot{\Omega}-\sigma g\frac{(\theta^4-1)}{(\theta_{af}^4-1)} \tag{17}$$

where the rescaled velocity and reaction rate are $V=v/\varepsilon^{1/2}$ and $\dot{\Omega}=\dot{\omega}/\varepsilon^{3/2}$ and stoichiometry and heat-release parameters of order unity are

$$S=\sqrt{\varepsilon}s, \qquad Q=\sqrt{\varepsilon}q \tag{18}$$

respectively. Equation (18) indicates that, along with s being large, q also is large, which is typical inasmuch as the heat release is large compared with the thermal enthalpy in the ambient atmosphere; the ordering in Eq. (18) defines a distinguished limit worthy of study, with small Q representing a limit in which there are significant simplifications, corresponding to combustion in a very hot ambient atmosphere, the chemistry having only a small influence on the temperature profile.[7] From the velocity scaling, with v of order $\sqrt{\varepsilon}$, the radial velocities in the outer zone are small compared with the maximum Stefan flow velocity near the droplet surface, but changes in this small velocity are significant, as induced by fractional density changes of order unity, resulting from fractional temperature changes of order unity. In this distinguished limit, then, convection remains in the outer zone at leading order in Eqs. (15–17), precluding the writing of explicit integral expressions for the solution as was done earlier[2] and necessitating a numerical approach.

As X approaches zero, the diffusion terms in Eqs. (15–17) become dominant, as do such terms in the quasisteady inner-zone equations as x approaches infinity. The matching region, thus, is a diffusively dominated quasisteady region at leading order. The quasisteady solution of Eqs. (12) and (13) was obtained by integrating inner-zone equations

$$\frac{\lambda}{fx^2}=\frac{\mathrm{d}\theta}{\mathrm{d}x}\Big/\left(\theta+l-\frac{a^2q'}{\lambda}-\theta_l\right)$$
$$=-\frac{\mathrm{d}Y_F}{\mathrm{d}x}\Big/Le_F(1-Y_F)=\frac{\mathrm{d}y_O}{\mathrm{d}x}\Big/Le_O y_O \tag{19}$$

When Eq. (19) is multiplied by fx^2 and written in outer variables, the matching conditions for the diffusive fluxes as X approaches zero are found to be

$$X^2\frac{f}{Le_F}\frac{\partial y_F}{\partial X}\to-\lambda, \quad \text{as} \quad X\to 0 \tag{20}$$

$$X^2\frac{f}{Le_O}\frac{\partial y_O}{\partial X}\to y_{Oa}\lambda, \quad \text{as} \quad X\to 0 \tag{21}$$

$$X^2 f\frac{\partial\theta}{\partial X}\to\sqrt{\varepsilon}\left(\theta_a+l-\frac{a^2q'}{\lambda}-\theta_s\right)\lambda, \quad \text{as} \quad X\to 0 \tag{21}$$

The earlier stated boundary conditions at infinity can be written in outer variables in the form $y_F\to y_O-1\to\theta-1\to 0$ as $X\to\infty$. Solution of Eqs. (14–17) with $\varrho\theta=1$, subject to these boundary conditions and those in Eqs. (20–22), determines the outer solutions as well as y_{Oa} and θ_a. In the Burke–Schumann limit, the flame sheet is located at $X=X_f$, of order unity. In that limit, there is no oxidizer inside the flame, $y_O=0$ for $X<X_f$, and so $y_{Oa}=0$ in Eqs. (12) and (21). With finite-rate chemistry, there is some oxygen leakage, and consequently y_{Oa} is not zero, but it is sufficiently small (prior to flame extinction) that y_{Oa} is negligibly small, enabling the right-hand side of Eq. (21) to be put to zero, avoiding the $1/X$ type of singularity. Equation (20) indicates that such a singularity is necessarily present in y_F for it to match. In Eq. (22), the right-hand side is seen to be of higher order in ε, so that, to leading order, Eq. (22) requires any singularity in θ as $X\to 0$ to be weaker than $1/X$. The matching of the temperature itself in fact requires that there be no singularity and that $\theta\to\theta_a$ as $X\to 0$.

It may be noted from Eq. (10) that, because $X_f=\sqrt{(\varepsilon)}x_f$ is of order unity, the quantity q' is of order $\sqrt{\varepsilon}$ and, thus, is to be neglected at leading order in Eqs. (12), (13), and (22); the direct radiative enhancement of the droplet burning rate is of order $\sqrt{\varepsilon}$. The dominant effect of the radiation, therefore, is the radiant loss from the outer zone, appearing in Eq. (17), decreasing θ below θ_f as X decreases inside the flame. For Lewis numbers of unity and in the absence of the radiation, $\theta=\theta_f=\theta_{af}=\theta_a=$ const everywhere inside the flame in this outer region, when reactant leakage is negligible. This result continues to apply later even if the fuel Lewis number differs from unity, but if either of the other conditions is violated, θ varies inside the flame. That variation and the consequent value of θ_a are determined by the numerical solution of the outer problem, defined by Eqs. (14–17) and the boundary conditions for $X\to 0$ and ∞ just discussed. Even at leading order, radiant loss reduces θ_a and thereby decreases the burning rate through Eq. (13). With the present scaling, the leading-order effect of radiation on the droplet burning rate, therefore, is to decrease it through the reduction in the effective temperature of the ambient atmosphere seen by the quasisteady zone, through radiant loss from the transient zone; the increase in the burning rate from radiant energy input to the droplet is smaller by the factor $\sqrt{\varepsilon}$, even for the optimum situation in which all of the radiation falling on the liquid is absorbed instantaneously. This result, associated with the geometrically small angle subtended by the droplet when the flame is in the outer zone, may not have an appreciable influence on the burning rate, however, because the decrease in θ_a is small numerically unless σ of Eq. (1) is large numerically, as will be seen.

Burke–Schumann Limit

Irrespective of the character of the asymptotic description of the reaction rate $\dot{\Omega}$, the Burke–Schumann flame-sheet approximation is recovered at leading order in the expansion. The Burke–Schumann problem, therefore, needs to be solved before further questions, such as the occurrence of flame extinction, can be addressed. This limit also provides, at leading order, the history of the flame location $X_f(\tau)$, for comparison with results of experiments.[4] In this well-known limit, $y_O=0$ for $X<X_f$ and $y_F=0$ for $X>X_F$, there being jump conditions on gradients of y_O, y_F, and θ at $X=X_F$, readily derivable from Eqs. (15–17) by letting $\dot{\Omega}$ approach a delta function.

The solution in this limit is best found by generalized Schvab–Zel'dovich variables[14]:

$$H=\frac{(\hat{S}+1)Le_F}{Q}\theta+y_O+y_F, \qquad Z=\hat{S}y_F-y_O+1 \tag{23}$$

where $\hat{S} = SLe_O/Le_F$. Here Z is unity at the flame and larger than unity on the fuel side, in which region the fuel concentration and temperature are given by

$$y_F = (Z-1)/\hat{S}, \qquad \theta = [H-(Z-1)/\hat{S}]Q/[Le_F(\hat{S}+1)] \tag{24}$$

whereas on the oxidant side,

$$y_O = 1-Z, \qquad \theta = [H+(Z-1)]Q/[Le_F(\hat{S}+1)] \tag{25}$$

The differential equations obeyed by the functions H and Z are found from Eqs. (14–17) to be

$$\frac{\partial}{\partial\tau}\left[X^2\varrho\int_0^Z Le(u)\,du\right] + \frac{\partial}{\partial X}\left[X^2\varrho V\int_0^Z Le(u)\,du\right] = \frac{\partial}{\partial X}\left(X^2 f\frac{\partial Z}{\partial X}\right) \tag{26}$$

$$\frac{\partial}{\partial\tau}\left\{X^2\varrho\left[H+\int_0^Z N(u)\,du\right]\right\} + \frac{\partial}{\partial X}\left\{X^2\varrho V\left[H+\int_0^Z N(u)\,du\right]\right\} = \frac{\partial}{\partial X}\left(X^2 f\frac{\partial H}{\partial X}\right) + R \tag{27}$$

where $f = f(H, Z)$, $R = R(H, Z)$ is the radiation term, as a function of H and Z,

$$Le = \begin{cases} Le_F, & Z > 1 \\ Le_O, & Z < 1 \end{cases}$$

$$N = \begin{cases} \dfrac{Le_F - 1}{\hat{S}}, & Z > 1 \\ (1 - Le_O), & Z < 1 \end{cases} \tag{28}$$

From Eqs. (17), (23), and (27), it is seen that

$$R = \frac{(\hat{S}+1)Le_F\sigma g(\theta^4 - 1)}{Q(\theta_{af}^4 - 1)} \tag{29}$$

The boundary conditions at zero for Eqs. (26) and (27), from Eqs. (20–22), are

$$X^2 f\frac{\partial Z}{\partial X} \to -\hat{S}Le_F\lambda, \quad \text{as} \quad X \to 0 \tag{30}$$

$$X^2 f\frac{\partial H}{\partial X} \to -Le_F\lambda, \quad \text{as} \quad X \to 0 \tag{31}$$

both functions exhibiting $1/X$ types of singularities. Boundary conditions at infinity are

$$Z \to H - (\hat{S}+1)Le_F/Q - 1 \to 0, \quad \text{as} \quad X \to \infty \tag{32}$$

Initial conditions are taken for all $X > 0$ to be

$$Z = H - (\hat{S}+1)Le_F/Q - 1 = 0, \quad \text{at} \quad \tau = 0 \tag{33}$$

the same as the conditions at infinity because the ignition impulse, which is assumed to lead rapidly to the establishment of the Burke–Schumann flame, is considered to be applied only in the inner zone near the droplet and not to produce excess fuel vapor in the outer zone. Different selections of initial conditions would lead to different solutions, but such solutions are found to approach those of the present problem with increasing τ. Equations (24–33), along with Eqs. (13) (with $q' = 0$ and evaluated at $x = \infty$, $\theta = \theta_a$) and (14), $\varrho\theta = 1$ and specifications of the functions f and g, and values of the constants fuel Lewis number Le_F, oxidizer Lewis number Le_O, S, Q, $l - \theta_l$, and σ define a well-posed initial/boundary-value problem for determining the twice continuously differentiable functions $Z(X, \tau)$ and $H(X, \tau)$, along with the functions $\theta_a(\tau)$ and $\lambda(\tau)$, in the domain $X > 0$, $\tau > 0$.

Solutions Without Radiant Loss

The problem without radiation and with an oxidizer Lewis number of unity has been treated by Fachini.[5] In this case, it is useful to consider the function $J \equiv H - Z/\hat{S}$, proportional to $\theta/Q + y_O/S$ according to Eq. (23). Equations (30) and (31) imply that $X^2 f\partial J/\partial X \to 0$ as $X \to 0$, that is, the flux of this function at the origin is zero. In addition, for $Le_O = 1$, from Eqs. (26–28) it can be shown that

$$\frac{\partial}{\partial\tau}(X^2\varrho J) + \frac{\partial}{\partial X}(X^2\varrho V J) = \frac{\partial}{\partial X}\left(X^2 f\frac{\partial J}{\partial X}\right) + R \tag{34}$$

both inside and outside the flame. In view of Eq. (14), when $R = 0$, the solution to Eq. (34) lacking the singularity at the origin is $J = \text{const}$. Application of Eq. (32) determines this constant, giving $H - Z/\hat{S} = 1 + (\hat{S}+1)Le_F/Q$, an explicit coupling of θ and y_O, in view of Eq. (23). Evaluation at the flame, where $y_O = 0$, gives from Eq. (23) the nondimensional flame temperature $\theta_f = 1 + Q/S = \theta_{af}$, the adiabatic flame temperature independent of the value of fuel Lewis number Le_F. The flame temperature is determined by the oxidizer–temperature balance and is unaffected by the rate of fuel diffusion.

Because $y_O = 0$ everywhere inside the flame, it in fact follows from Eq. (23) that $\theta = \theta_{af}$ throughout the region $X \le X_f$, so long as $R = 0$ everywhere and $Le_O = 1$. That is, in the absence of any radiant energy loss, the temperature is constant and equal to the adiabatic flame temperature throughout the fuel zone ($0 < X < X_f$), irrespective of the value of fuel Lewis number Le_F, when $L_O = 1$, resulting in λ/a constant from Eq. (13), as already explained. With $R = 0$ everywhere and $L_O = 1$, the value of fuel Lewis number Le_F does affect the flame location X_f, even though it has no influence on θ_f. This occurs because fuel Lewis number Le_F determines the rate at which fuel can diffuse into the reaction sheet. Representative results for $X_f(\tau)$ with $R = 0$ and $L_O = 1$ for three different fuel Lewis numbers, as obtained from the numerical integration (Appendix B) are shown in Fig. 1. Figure 1 demonstrates that a higher fuel diffusion coefficient (a smaller value of fuel Lewis number Le_F) causes a larger diffusion velocity, with the flame moving away from the droplet more rapidly when traveling outward and moving back more rapidly when traveling inward. Although the effect of fuel Lewis number Le_F is small in Fig. 1, it is large under some other conditions,[5] for example, at larger values of S.

Even when $L_O \neq 1$, working with J, as earlier described, shows from Eqs. (26–33) that Eq. (34) still applies for $X < X_f$, and $X^2 f(\partial J/\partial X) \to 0$ as $X \to 0$, consistent with J being constant inside the flame when $R = 0$; that is, $H - Z/\hat{S} = \text{const}$ is a solution for $0 < X < X_f$ for any fuel Lewis number in the absence of radiation, resulting (through Eq. (23) with $y_O = 0$) in $\theta = \theta_f = \text{const}$ for $0 < X < X_f$. The initial condition of Eq. (33) then gives

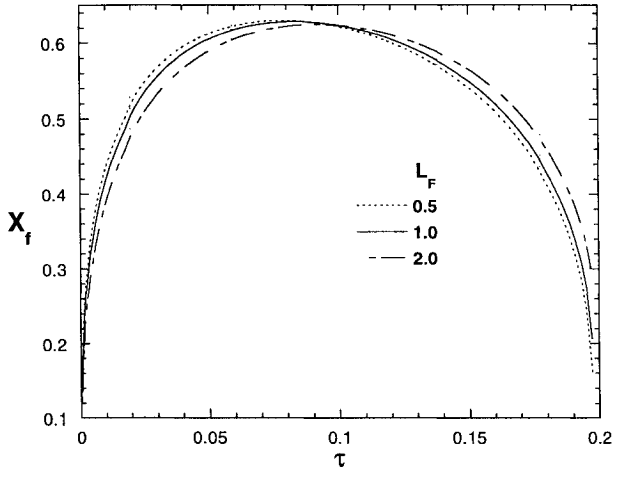

Fig. 1 Dependence of the nondimensional flame position on the nondimensional time for different values of the fuel Lewis number, without radiation ($\sigma = 0$), with an oxidizer Lewis number of unity ($Le_O = 1$), and with the representative stoichiometry $S = 1$ and nondimensional heat release $Q = 5$.

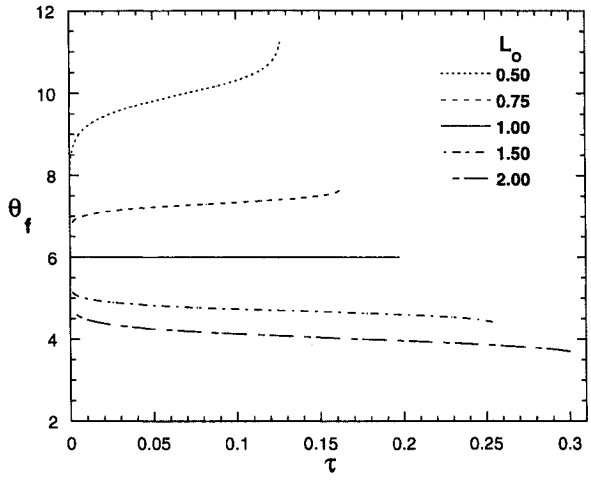

Fig. 2 Evolution of the nondimensional flame temperature for different value of the oxidizer Lewis number, without radiation ($\sigma = 0$), and with the representative fuel Lewis number $Le_F = 1$, stoichiometry $S = 1$, and nondimensional heat release $Q = 5$.

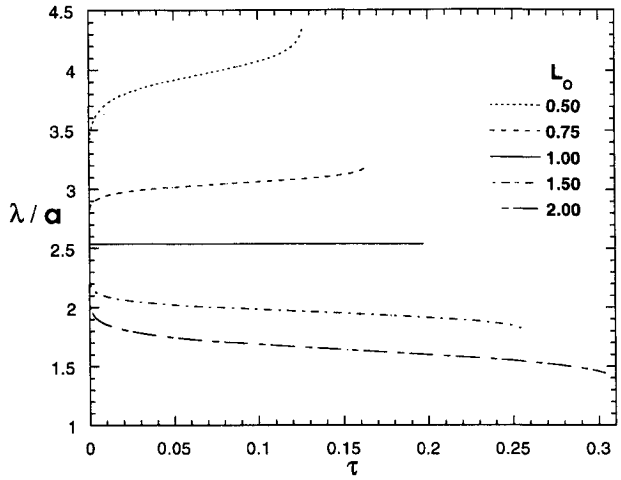

Fig. 3 Variation of the burning-rate constant λ/a with the nondimensional time for different oxidizer Lewis numbers, without radiation ($\sigma = 0$), and with the representative fuel Lewis number $Le_F = 1$, stoichiometry $S = 1$, and nondimensional heat release $Q = 5$.

$J = 1 + (\hat{S} + 1)Le_F/Q$, corresponding to $\theta_f = 1 + Q/(SLe_O)$, the adiabatic value, θ_{af}, only for $Le_O = 1$. This simple solution has $\theta_f > \theta_{af}$ for $Le_O < 1$ and $\theta < \theta_{af}$ for $Le_O > 1$, results again leading to $\lambda/a = \text{const}$ from Eq. (13) irrespective of the value of the fuel Lewis number when $R = 0$ and consistent with expectations from considering the oxidizer region $X > X_f$. For $Le_O < 1$, the diffusivity of the oxidizer exceeds that of heat, and therefore, to maintain the convective–diffusive enthalpy balance in the region $X_f < X < \infty$, it is necessary that $\theta_f > \theta_{af}$, giving a superadiabatic flame temperature. Conversely, for $Le_O > 1$, subadiatic flame temperatures, $\theta_f < \theta_{af}$, are obtained.

This simple situation, however, is not attained because the differential equations and boundary conditions in the region $X > X_f$ effectively apply a boundary condition on Eq. (34) at $X = X_f$ that is not consistent with θ_f being independent of τ and J being constant inside the flame. Representative results of numerical integrations for different Lewis number of the oxidizer, without radiation, as shown in Fig. 2, demonstrate increasing departure of θ_f from θ_{af} with increasing τ, for a case in which $\theta_{af} = 6$, but qualitative results inferred earlier, such as $\theta_f > \theta_{af}$ for $Le_O < 1$ and $\theta_f < \theta_{af}$ for $Le_O > 1$, remain valid. Quite rapidly θ_f departs from its initial value $\theta_{af} + (Q/S)(1 - Le_O)/Le_O$ and achieves a different value, dependent on oxidizer Lewis number Le_O, that varies slowly with time thereafter, although there is stronger variation just before the droplet disappears. These changes are associated with the variation the flame position X_f and are most rapid when X_f is small; they arise from the effectively adiabatic condition at the origin and the heat-release condition at the flame, which ultimately imposes the flame-temperature variation. Figure 3 shows the corresponding variation of the vaporization-rate constant λ/a, which is also slight; after the initial rapid departure from the value associated with the initial value of θ_f (2.534 in the case $Le_O = 1$), λ/a is nearly constant until the droplet nearly disappears. Figure 4, obtained from Fig. 3 by using Eq. (11), shows that the resulting departures from the classical diameter-squared law are barely perceptible. The associated histories of the flame position, shown in Fig. 5, illustrate how increasing the diffusion coefficient of the oxidizer (decreasing oxidizer Lewis number Le_O) substantially reduces both maximum flame radius and nondimensional burning time, by bringing the oxidizer more rapidly to the flame.

Solutions with Radiant Loss

The effect of radiation in the Burke–Schumann limit can be seen from the sequence of temperature profiles shown in Fig. 6 for different values of the normalized emissivity σ. There is no curve in Fig. 6 for $\sigma = 0$ at $\tau = 0.2$ because the absence of loss causes the combustion to be completed before $\tau = 0.2$. The dependence of R on temperature may be strong enough that $R = 0$ is a good approximation outside the flame even when there is a radiant loss from the

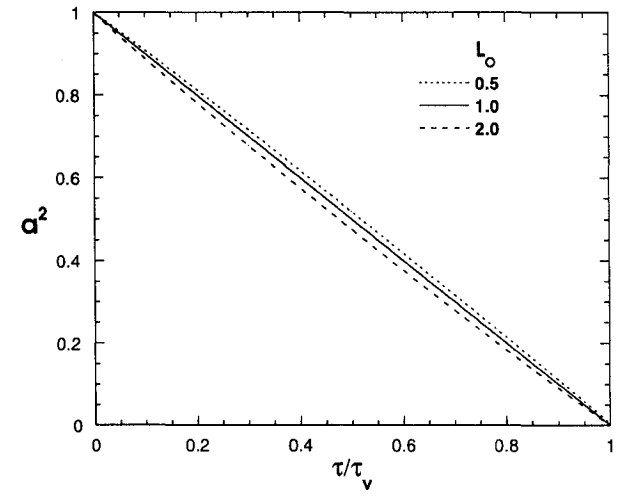

Fig. 4 Evolution of the square of the nondimensional droplet radius a for different values of the oxidizer Lewis number, without radiation ($\sigma = 0$) and with the representative values $Le_F = S = 1$, $Q = 5$; τ_v is the total droplet vaporization time.

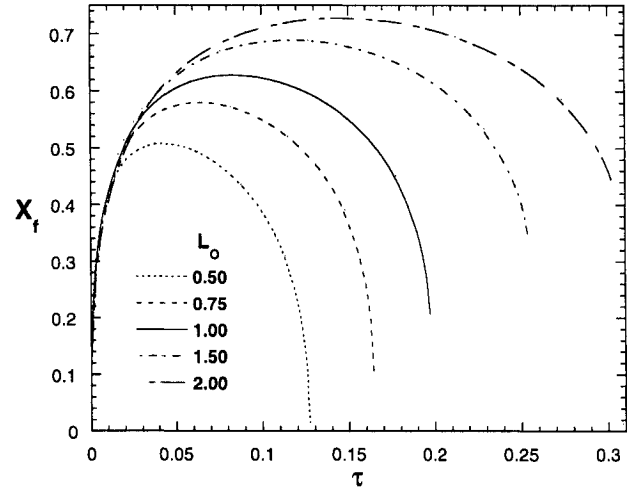

Fig. 5 Dependence of the nondimensional flame position on the nondimensional time for different values of the oxidizer Lewis number, without radiation ($\sigma = 0$), with a fuel Lewis number of unity ($Le_F = 1$) and with the representative stoichiometry $S = 1$ and nondimensional heat release $Q = 5$.

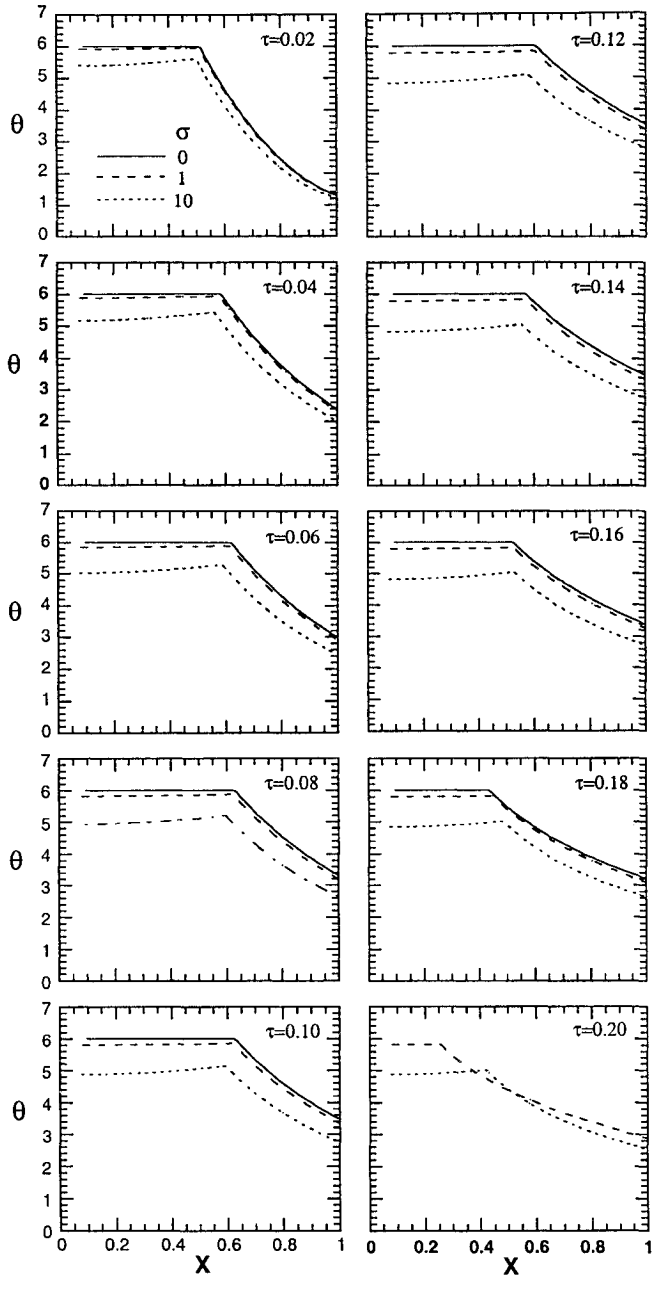

Fig. 6 Effect of the radiant loss parameter σ on the temperature profile for different values of the nondimensional time τ, with the representative values $Le_F = Le_O = S = 1$, $Q = 5$ for the other parameters in the Burke–Schumann limit.

hot zone $X \leq X_f$, giving the approximate last expression in Eq. (10), although this approximation was not used in generating Fig. 6. The radiant loss from the zone $X \leq X_f$ causes a decrease in temperature with decreasing X, the value $\theta_a < \theta_f$ being approached as $X \to 0$. The radiation also causes θ_a and θ_f to depend on τ.

Figure 6 shows that there is little effect of radiation even for σ of unity; σ must approach 10 or larger to achieve a noticeable peak of temperature at the flame. Oxidizer Lewis numbers less than unity also can produce a temperature peak at the flame, but this effect also is mild, and so appreciably large values of σ always are necessary to produce the temperature peak required for abrupt rather than gradual extinction.

Variations of the nondimensional flame temperature θ_f, the nondimensional burning-rate constant λ/a, and the nondimensional flame radius X_f, with the nondimensional time τ, are shown in Figs. 7, 8, and 9, respectively, for the conditions of Fig. 6. It is seen, as expected, that the radiant energy loss reduces the flame temperature, the burning rate, and the maximum flame radius, the last of these because of the reduced burning rate and the increased gas density

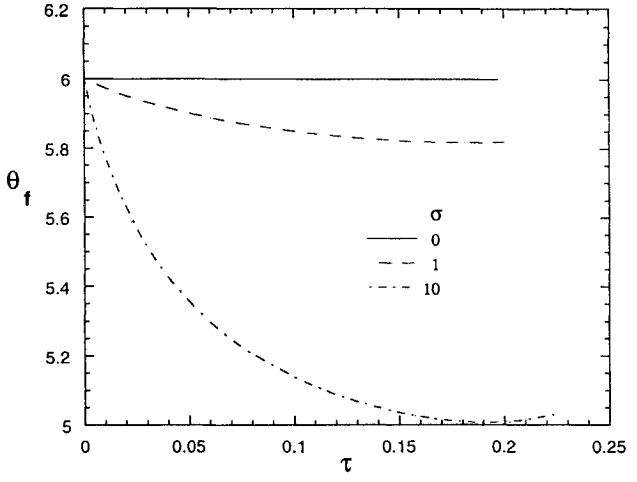

Fig. 7 Evolution of the nondimensional flame temperature for different values of the radiation parameter σ, with representative values $Le_F = Le_O = S = 1$, $Q = 5$ for the other parameters in the Burke–Schumann limit.

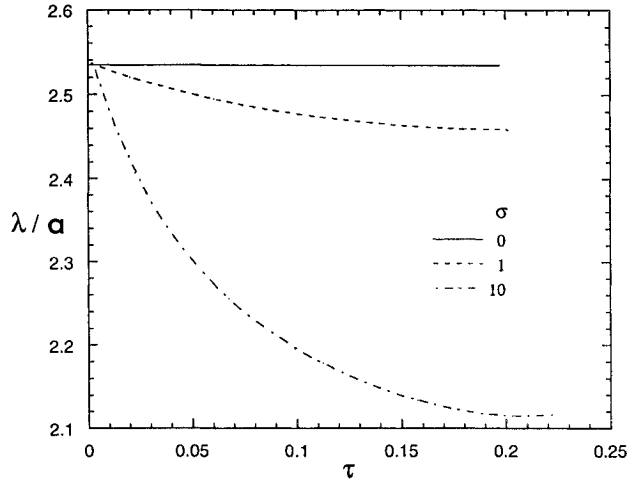

Fig. 8 Variation of the burning-rate constant λ/a with the nondimensional time τ for different values of the radiation parameter σ, with representative values $Le_F = Le_O = S = 1$, $Q = 5$ for the other parameters in the Burke–Schumann limit.

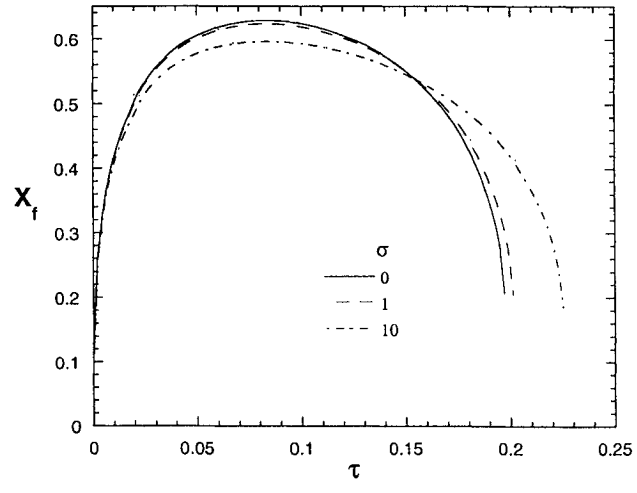

Fig. 9 Dependence of the nondimensional flame radius on the nondimensional time τ for different values of radiation parameter σ, with representative values $Le_F = Le_O = S = 1$, $Q = 5$ for the other parameters in the Burke–Schumann limit.

inside the flame. The radiant loss causes the flame temperature and burning rate to decreases with time, producing more curvature in Fig. 4 like that for $Le_O > 1$. A small increase in θ_f with time is seen at the end of the curve for $\sigma = 10$ in Fig. 7; this is associated with the rapidly decreasing flame radius reducing the volume from which radiant energy is lost and thereby reducing the total loss, and it leads to the slight increase in the burning-rate constant at the end of the corresponding curve in Fig. 8. At the beginning of the curves in Fig. 8, it may be noted that the burning-rate constant increases slightly with σ; this occurs because, to illustrate influences of absorption of radiant energy by the liquid, the computations included q' in Eq. (13), employing $\varepsilon = 10^{-3}$ and $g = 1$ in Eq. (10). This shows that, at reasonable density ratios, the influence of absorption of radiant energy by the droplet is quite small when the flame is in the outer zone.

Analysis of Flame Extinction

To address the flame extinction, the structure of the reaction zone must be considered. The present study employs one-step activation-energy asymptotics for this purpose. The rate of consumption of fuel per unit volume is, thus, taken to be

$$\omega_F = A_F \rho y_O^{m_1} Y_F^{m_2} e^{-E/R^0 T} \tag{35}$$

where E is the constant activation energy, R^0 is the universal gas constant, m_1 and m_2 are the constant reaction orders with respect to oxidizer and fuel, respectively, and A_F is a constant prefactor with units of reciprocal time. Any temperature variations of the pre-exponential Arrhenius factor that would cause A_F to vary have been included here as a small contribution to E through expansion about the flame temperature. Although explicit results are available only for $m_1 = m_2 = 1$, the initial formulation is given here for arbitrary reactions orders because it is simple and could be of future interest.

With this reaction-rate expression, the definitions of $\dot{\omega}$ and $\dot{\Omega}$ yield

$$\dot{\Omega} = Da \rho y_O^{m_1} y_F^{m_2} \exp[-\beta(\theta_{af}/\theta - 1)] \tag{36}$$

where the nondimensional activation energy is $\beta = E/(R^0 T_{af})$ and a Damköhler number

$$Da = \frac{a_0^2 A_F Y_{O\infty}^{m_1} e^{-\beta}}{\alpha_\infty \varepsilon^{(3-m_2)/2}} \tag{37}$$

The flame structure is treated by considering the limit $\beta \to \infty$, following Liñán's analysis of the counterflow diffusion flame,[8] as applied to quasisteady droplet combustion by Law[15] and extended to Lewis numbers different from unity by Chung and Law[16] and by Liñán and Rodrigues,[17] with further extension by Fachini.[18]

Because $\sqrt{\varepsilon}$ is the small parameter in the present analysis, it is mathematically most transparent to treat $\gamma = \theta_f^2/(\beta\theta_{af})$ as being of order $\sqrt{\varepsilon}$ in the asymptotic analysis for $\beta \to \infty$, but this is not really necessary because the same results are obtained irrespective of the ordering. The expansions adopted, therefore, are

$$\begin{aligned} \theta &= \theta_f - \gamma\delta^{-1/(1+m_1+m_2)}(\Theta + m\xi) + \mathcal{O}(\gamma) \\ y_O &= \gamma\Psi_O + \mathcal{O}(\gamma), \qquad y_F = \gamma\Psi_F + \mathcal{O}(\gamma) \\ Z &= 1 + \gamma z + \mathcal{O}(\gamma), \qquad H = H_f + \gamma h + \mathcal{O}(\gamma) \end{aligned} \tag{38}$$

where the stretched spatial variable is

$$\xi = \frac{c(X - X_f)}{\gamma} \tag{39}$$

the constant c being chosen (Appendix C) to achieve unity heat loss in the transformed problem. The values of m and δ are selected to simplify the formulation of the extinction problem. The term $m\xi$ causes a rotation in the problem, to equalize the heat conduction to the two sides of the flame in the transformed variables. The

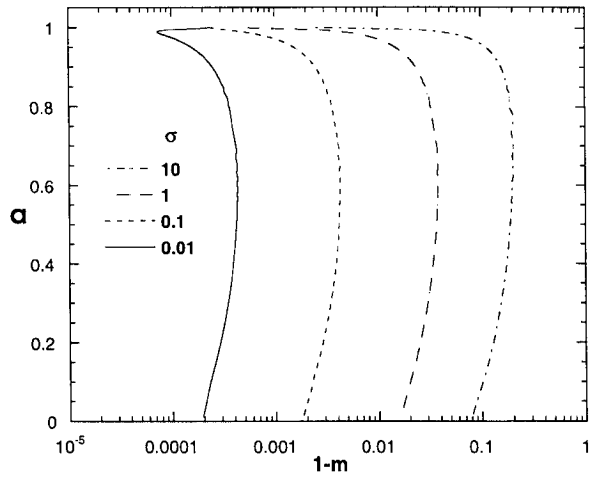

Fig. 10 Variation of the nondimensional droplet radius with $1 - m$ for different values of the radiation parameter σ, with representative values $Le_F = Le_O = S = 1$ and $Q = 5$.

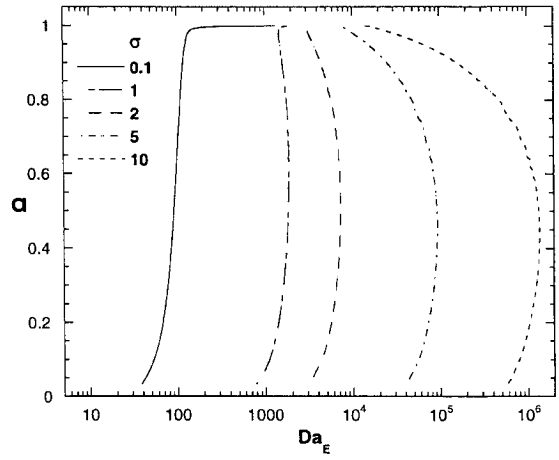

Fig. 11 Variation of the nondimensional droplet radius with the extinction Damköhler number for different values of the radiation parameter σ, with representative values $Le_F = Le_O = S = 1$, $Q = 5$, and $\beta = 30$.

parameter δ is a reduced Damköhler number (Appendix C). The flame-structure problem becomes

$$\frac{d^2\Theta}{d\xi^2} = (\Theta + \xi)^{m_1}(\Theta - \xi)^{m_2}\exp\left[-\delta^{-1/(1+m_1+m_2)}(\Theta + m\xi)\right] \tag{40}$$

$$\begin{aligned} \frac{d\Theta}{d\xi} &\to -1, \quad \text{as} \quad \xi \to -\infty \\ \frac{d\Theta}{d\xi} &\to 1, \quad \text{as} \quad \xi \to \infty \end{aligned} \tag{41}$$

from which $\Theta(\xi)$ is found for given values of m_1, m_2, m, and δ. There are two solutions for $\delta > \delta_E$ and none for $\delta < \delta_E$, where $\delta_E(m_1, m_2, m)$ is the reduced Damköhler number for extinction.[8] This results in an expression for the extinction Damköhler value Da_E of the Damköhler number Da of Eq. (37). An expression for extinction Damköhler number Da_E is given in Appendix C.

The equations in Appendix C enable m and extinction Damköhler number Da_E to be obtained from the numerical Burke–Schumann solutions. It is convenient to exhibit these results as functions of the nondimensional radius a instead of τ. Figure 10 shows a as a function of $1 - m$ for various values of the heat-loss parameter σ, for $Le_O = Le_F = S = 1$ and $Q = 5$. It is seen in Fig. 10 that $1 - m$ is small even for σ as large as 10, thereby indicating that the simplified extinction result of Appendix C is quite accurate. For this same representative case, Fig. 11 shows the nondimensional droplet radius as a function of the extinction Damköhler number. Unlike the value of the m, the value of the extinction Damköhler number Da_E

depends on the value of the nondimensional activation energy β, and therefore, Fig. 11 would be different for different values of β. Figure 11 is especially relevant to radiative extinction phenomena.

According to Eq. (37), each droplet combustion experiment corresponds to a particular Damköhler number Da, determined by the fuel, the atmosphere, the adiabatic flame temperature, the molecular transport and reaction-rate parameters, and the initial droplet size. For the flame to exist, this constant Damköhler number Da must exceed the extinction Damköhler value Da_E, which varies during combustion because of variations in the nondimensional flame temperature θ_f and nondimensional gradients at the flame (b_Z and b_H). When the radiant heat-loss parameter σ is sufficiently small, as in the curve for $\sigma = 0.1$ in Fig. 11, extinction Damköhler number Da_E decreases monotonically with time during burning, as a decreases, implying that if initially the flame can be established ($Da > Da_E$ at $a = 1$), then it continues to exist until the droplet disappears ($Da > Da_E$ for all $a > 0$). For these small radiant losses, radiant extinction cannot occur, and flame extinction then never occurs before the droplet vanishes if the flame is in the outer zone. If the flame were in the inner (quasisteady) zone, then diffusive extinction could occur, but diffusive extinction never occurs with the droplet present when the flame is in the outer zone. After the droplet disappears, the flame radius will contract rapidly, and diffusive extinction eventually will occur. Sufficiently extensive analyses of histories subsequent to droplet disappearance have not been performed, although analyses without radiation for an oxidizer Lewis number of unity are available.[5]

At higher values of the radiant heat-loss parameter σ, as seen in the curves for $\sigma = 2$–10 in Fig. 11, the extinction Damköhler number Da_E first increases with time, reaches a maximum, then decreases as the droplet size approaches zero. The increase is associated mainly with the factor $\exp(\beta\theta_{af}/\theta_f) = \exp(E/R^0T_f)$ in Eq. (C9), because the increasing flame radius increases the radiant loss and thereby decreases the flame temperature T_f, producing a large effect on the extinction Damköhler number Da_E at high activation energy. If the Damköhler number Da is greater than the initial value of the extinction Damköhler number Da_E but less than its maximum value, this increase in the extinction Damköhler number Da_E causes the flame to extinguish at some point in its burning history, corresponding to radiative extinction. In this range of conditions, the larger the Damköhler number Da is, the later the flame extinguishes in its history. It is of interest to observe that, at the larger values of Damköhler number Da, radiative extinction can occur well after the flame has passed through its maximum radius. This is observed experimentally[4] and is possible because the maximum value of the extinction Damköhler number Da_E occurs after the maximum of X_f; the value of θ_f continues to decrease through radiant loss (see Fig. 7) well after X_f has passed its maximum (Fig. 9), resulting in the continuing increase in the extinction Damköhler number Da_E from Eq. (C9). In term of droplet radius, for $\sigma \geq 2$ the maximum of the extinction Damköhler number Da_E occurs at approximately $a = 0.45$, as seen in Fig. 12, indicating that, if there is extinction, at least $\frac{1}{8}$ of the mass of the droplet does not burn. At smaller values of the Damköhler number Da, radiative extinction occurs before the flame achieves its maximum radius, and, of course, if the Damköhler number Da is too small, then radiative extinction already would occur at the initial condition, and combustion is impossible, that is, $a_E = 1$, as shown in Fig. 12.

The ratio Da/Da_E may be evaluated from Eq. (37) and Appendix C. Because this ratio must exceed unity to avoid flame extinction, an explicit criterion for radiative extinction can be extracted. The criterion in general appears somewhat complicated because it involves the functions $b_Z(\tau)$ and $b_H(\tau)$, but simple estimates of these parameters, developed in Appendix D, enable a more transparent but very approximate expression to be obtained. The result is that combustion can occur only if the inequality

$$\frac{3l_{Paf}Le_F c_p T_f \rho_f Y_{O\infty} A_F \exp[-E/(R^0T_{af})]}{2e\lambda^2\sigma_B(T_{af}^4 - T_\infty^4)(\rho_\infty/\rho_l)[Q_F/(c_pT_\infty)]^2[E/(R^0T_{af})]} > 1 \tag{42}$$

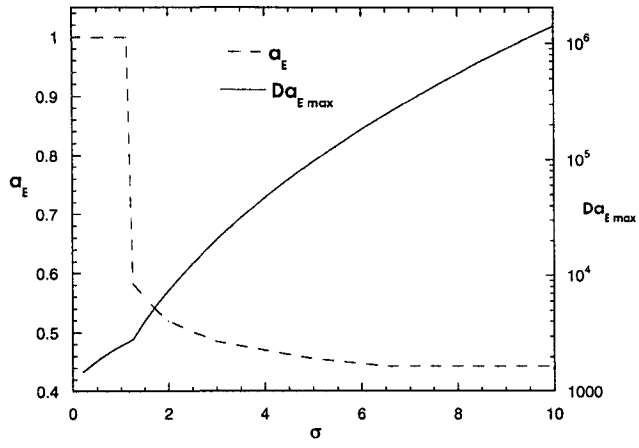

Fig. 12 Maximum of the extinction Damköhler number and the corresponding value of the nondimensional droplet radius as functions of the radiation parameter σ, with representative values $Le_F = Le_O = S = 1$, $Q = 5$, and $\beta = 30$.

is satisfied. Equation (42) states in general that the heat-release rate must be sufficiently large in comparison with the radiant-loss rate to avoid extinction. This can be exhibited more explicitly by writing Eq. (42) in the form

$$\frac{c_pT_f\rho_fY_{O\infty}A_Fe^{-E/(R^0T_{af})}}{\sigma_B(T_{af}^4 - T_\infty^4)/l_{Paf}} > \frac{25}{6}\frac{E}{R^0T_{af}} \tag{43}$$

where it has been observed that $[Q_F\sqrt{(\rho_\infty/\rho_l)}/(c_pT_\infty)]$ is order unity and $\lambda = \frac{5}{2}$ according to Eq. (18) and Fig. 3, respectively.

Equation (42) is useful for rough quantitative estimates but is not a replacement for the more detailed computations, employing Eq. (C9), for accurate extinction calculations. In particular, memory effects leading to extinction at some time during the burning history are absent from Eq. (42) because it employs the quasisteady flame radius, which decreases with time. This is reflected by the factor λ^2 in the denominator in Eq. (42), which is proportional to the square of the ratio of the droplet radius to the initial droplet radius according to Fig. 3 and Eq. (13) evaluated at $x = \infty$, so that the equation predicts radiative extinction either initially or not at all. It is necessary to retain the variations of $b_Z(\tau)$, $b_H(\tau)$, and $\theta(\tau)$ to predict extinction during the combustion history. Thus, Eq. (42) is to be used only for order-of-magnitude estimates of whether radiative extinction may occur. If the inequality is strongly satisfied, then radiative extinction does not occur, but if it is violated, then such extinctions should be suspected. Within the accuracy of the equation, λ may be set equal to $\frac{5}{2}$ (see Fig. 3). The advantage of presenting the equation is that it exhibits explicitly the physical quantities that affect radiative extinction.

Conclusions

A rich variety of flame-history behaviors can occur during droplet combustion when the stoichiometric fuel–air ratio is small. The flame then lies in an outer region in which transient accumulation, convection, diffusion, and possibly also radiant energy loss all occur at leading order. The presence of so many phenomena necessitates numerical integration of the parabolic partial differential equations in this region even in the Burke–Schumann limit, with the inner quasisteady region providing singular boundary conditions at the origin through matching in a diffusion-dominated intermediate zone.

At these low stoichiometric fuel–air ratios, the ratio of the flame radius to the droplet radius is large, of the order of the stoichiometric air–fuel ratio and also of the square root of the ratio of the liquid density to the density of the ambient oxidizing gas. The flame radius increases with time, reaches a maximum value, then decreases with time when radiant energy loss can be neglected. The influence of radiation increases as the nondimensional emissivity parameter of Eq. (1) increases. When this parameter becomes large enough, radiant extinction occurs, first after and then before the flame reaches its maximum radius. Further increase in this parameter results in a

flammability-limit condition under which the outer-zone flame cannot be established at all because, if it were, the radiant losses would be too large. The radiant loss rate that is of greatest importance often occurs predominantly from the portion of the outer region inside the flame radius because this is the hottest region of the gas. The loss is distributed throughout this region and is not localized near the flame.

The flame-history and extinction results depend quantitatively on fuel and oxidizer Lewis numbers, scaled stoichiometric-ratio and heat-release parameters, other thermal parameters, the nondimensional emissivity parameter and, for extinction, a Damköhler number and nondimensional activation energy as well. Applications of the predictions to droplet-combustion experiments require evaluations of these parameters. Determination of effective values of the two overall Arrhenius reaction-rate parameters necessitates study of the combustion chemistry. Reduced-chemistry formulations are available that can be pursued to relate the effective Arrhenius reaction-rate parameters to elementary detailed chemical kinectics of combustion; this would be one appropriate direction for future research. The present results, in general, provide a description of flame histories and extinction in terms of a minimal number of nondimensional parameters.

Appendix A: Radiation Problem

A simple way to calculate the radiant energy received by the droplet when the flame is in the outer zone is to observe that the droplet is then small compared with all significant emitting radii. In spherical coordinates, with radius r, polar angle θ', and azimuthal angle φ, erected with the normal to the droplet surface element of interest in the polar direction, the energy per unit time emitted from a volume element is $(4/l_P)\sigma_B(T^4-T_\infty^4)\,\mathrm{d}r(r\,\mathrm{d}\theta')(r\sin\theta'\,\mathrm{d}\phi)$. This gives rise, at distance r, to the flux $(4/l_P)\sigma_B(T^4-T_\infty^4)\sin\theta'\,\mathrm{d}\theta'\,\mathrm{d}\phi\,\mathrm{d}r/(4\pi)$, resulting in an energy per unit normal surface area per unit time incident on the droplet surface element of $\cos\theta'$ times this. Integration over φ from 0 to 2π, θ' from $-\pi/2$ to $\pi/2$, and r from $r_{\min}$ to ∞ then gives for the total radiant energy flux at the droplet surface:

$$q' = \frac{2\sigma_B a_0}{\rho_\infty \alpha_\infty c_p T_\infty}\int_{r_{\min}}^{\infty}\frac{(T^4-T_\infty^4)}{l_P}\,\mathrm{d}r \tag{A1}$$

which yields Eq. (10) when use is made of Eq. (1).

When the droplet radius is not negligible compared with the radius of the regions from which radiation is emitted, a more classical and more involved analysis is needed, and the expression for the total radiant energy flux q' [Eq. (A1)] is modified because it includes geometrical effects of the droplet size and shape. The resulting expression is

$$q' = \frac{2\sigma_B a_0}{\rho_\infty \alpha_\infty c_p T_\infty}\int_a^\infty \frac{(T^4-T_\infty^4)}{l_P} \times \int_{\theta_i'}^{\pi-\theta_i'}\frac{(r\cos\theta'-a)(r-a\cos\theta')r^2\sin\theta'}{(r^2+a^2-2ra\cos\theta')^2}\,\mathrm{d}\theta'\,\mathrm{d}r \tag{A2}$$

where the angle θ_i' is $\arccos(a/r)$.

Appendix B: Numerical Considerations

The numerical integrations of Eqs. (14), (26), and (27) were performed by an explicit McCormack scheme.[19] The space variable X was replaced by the stream function ψ (as done previously by Cho et al.[20]) defined by $\partial\psi/\partial\tau = -X^2\varrho V$ and $\partial\psi/\partial X = X^2\varrho$, changing Eqs. (26) and (27) to a transient-heat-conduction problem plus a source term. For the solution of those equations to be stable[19] the quantity $X^4\varrho f\Delta\tau/\Delta\psi^2$ has to be less than 0.5. In the present computation, this quantity was 0.1. Because the value of this quantity varies strongly with X, this condition was satisfied by employing a grid with nonuniform steps defined by $(X-X_0)/(X_\infty-X_0)=P$, where $X_0=0$ and $X_\infty=10$ are the limits of the domain used in the computation, and $P=P_1\eta+(1-P_1)[1-\tanh(P_2(1-\eta))/\tanh P_2]$. Here η is assigned a uniform grid over the unit internal $(0\le\eta\le 1)$, and P_1 and P_2 control the nonuniformity of the grid[19]; the values employed for P_1 and P_2 were 10^{-4} and 7, respectively. This grid could be used because the temperature and oxidizer concentration vary slowly for $X>2$.

In the calculations, variations of the transport properties were approximated as $f=\sqrt{\theta}$, variations of the Planck-mean absorption length were neglected ($g=1$), and the heat of vaporization was put equal to the absolute thermal enthalpy at the droplet to reduce the number of parameters ($L_V = c_p T_l$, giving $l=\theta_l$). The results are only weakly sensitive to these selections, which are physically reasonable; for example, with the representative values $c_p=0.25$ cal/g K and $T_\infty=300$ K, methanol has the values 3.51 and 1.29 ethanol 2.68 and 1.13, n-heptane 1.01 and 1.23, and benzene 1.26 and 1.18 for the parameters l and θ_l, respectively.

Appendix C: Reaction-Zone Equations

Equations (15–17), written in the reaction-zone variables defined in Eqs. (38) and (39) describe the behavior of the oxidizer and fuel concentrations and of the temperature in the reaction zone, where there is a diffusive–reactive balance at leading order. Linear combinations eliminate reaction-rate terms to provide coupling-function solutions

$$\hat{S}\Psi_F - \Psi_O = -b_Z\xi/c \tag{C1}$$

$$-\frac{(\hat{S}+1)Le_F}{Q}\frac{(\Theta+m\xi)}{\delta^{1/(1+m_1+m_2)}} + \Psi_F + \Psi_O = -\frac{b_H\xi}{c} \tag{C2}$$

where

$$b_H(\tau) \equiv \left|\left(\frac{\partial H}{\partial X}\right)_{X=X_f}\right|, \qquad b_Z(\tau) \equiv \left|\left(\frac{\partial Z}{\partial X}\right)_{X=X_f}\right| \tag{C3}$$

It is thereby found from Eqs. (C1) and (C2) that the expressions

$$\Psi_F = \frac{Le_F}{Q\delta^{1/(1+m_1+m_2)}}(\Theta-\xi) \tag{C4}$$

$$\Psi_O = \frac{\hat{S}Le_F}{Q\delta^{1/(1+m_1+m_2)}}(\Theta+\xi) \tag{C5}$$

are obtained after introducing the definitions

$$m = 1 - 2(1-\hat{S}b_H/b_Z)/(1+\hat{S}) \tag{C6}$$

$$c = Qb_Z\delta^{1/(1+m_1+m_2)}/(2\hat{S}Le_F) \tag{C7}$$

$$\delta = 4\left(\theta_f^2/\beta\theta_{af}\right)^{m_1+2m_2-2}Da\varrho_f\exp[-\beta(\theta_{af}/\theta_f-1)] \times Le_F^{m_2}(SLe_O)^{2+m_1}/\left(Q^{1+m_1+m_2}\theta_f^{1+n}b_Z^2\right) \tag{C8}$$

The remaining equation from Eqs. (15–17), containing the chemical source term, then provides Eqs. (40) and (41) after transformation and matching.[8]

The solution to the problem in Eqs. (40) and (41) has been obtained previously[8] for $m_1=m_2=1$. An expression may be found[8] for δ_E as a function of m. In the present problem, $1-m$ is small, as seen in Fig. 10, simplifying the expression for δ_E. Use of this simplified expression[8] and of Eqs. (C6) and (C7) in Eq. (C8) enables the extinction Damköhler number Da_E to be written as

$$Da_E = \frac{b_Z(b_Z-\hat{S}b_H)}{2(1+\hat{S})}\frac{Q^3\theta_f^{\frac{3}{2}}\exp[1+\beta(\theta_{af}/\theta_f-1)]}{Le_F(SLe_O)^3}\frac{\beta\theta_{af}}{\theta_f} \tag{C9}$$

Appendix D: Simplifications for Estimating Extinction Damköhler Numbers

Transient and convective terms may be neglected to obtain rough estimates of the coefficients b_Z and b_H of Appendix C. If, in addition, the transport-coefficients and radiation terms are taken to be constant

and equal to their values at the flame, the problem specified by Eqs. (26–33) reduces to

$$\frac{\mathrm{d}}{\mathrm{d}X}\left(X^2 f_f \frac{\mathrm{d}Z}{\mathrm{d}X}\right) = 0 \tag{D1}$$

$$\frac{\mathrm{d}}{\mathrm{d}X}\left(X^2 f_f \frac{\mathrm{d}H}{\mathrm{d}X}\right) = X^2 R_f \tag{D2}$$

where $f_f = \sqrt{\theta_{\mathrm{af}}}$ and $R_f = (\hat{S}+1)Le_F\sigma/Q$. Integrating Eqs. (D1) and (D2) with the boundary conditions of Eqs. (30–32) gives for b_Z and b_H, through Eqs. (C3),

$$b_Z = \frac{\hat{S}\lambda Le_F}{f_f X_f^2} \tag{D3}$$

$$b_H = \frac{\lambda Le_F}{f_f X_f^2} - \frac{X_f^3 R_f}{3 f_f} \tag{D4}$$

The solution of Eq. (D1) at the flame ($Z = 1$ at $X = X_f$), gives the flame position

$$X_f = \frac{\hat{S}\lambda Le_F}{f_f} \tag{D5}$$

which leads to

$$b_Z = \frac{\sqrt{\theta_{\mathrm{af}}}}{SLe_O\lambda} \tag{D6}$$

$$b_H = \frac{Le_F\sqrt{\theta_{\mathrm{af}}}}{(SLe_O)^2\lambda} - \frac{SLe_O\lambda R_f}{3\theta_{\mathrm{af}}} \tag{D7}$$

These approximate values for b_Z and b_H were used to obtain Eq. (42). Although potentially very inaccurate with the flame in the outer transient zone, the result may nevertheless be useful for estimating extinction conditions because Eq. (C9) is not exceedingly strongly dependent on b_Z and b_H, the dominant variable factor being the Arrhenius factor.

Acknowledgments

This work was supported in part by the Conselho Nacional de Desenvolvimento Científico e Tecnológico–CNPq under Grant 200554/87-5 and in part by the NASA Microgravity Combustion Reseach Program through NASA John H. Glenn Research Center at Lewis Field. The first author thanks Fred Dryer, Vedha Nayagam, and Paul Ronney for discussions of influences of radiant loss.

References

[1]Williams, F. A., *Combustion Theory*, 2nd ed., Addison–Wesley, Redwood City, CA, 1985, pp. 52–69.

[2]Crespo, A., and Liñán, A., "Unsteady Effects in Droplet Evaporation and Combustion," *Combustion Science and Technology*, Vol. 11, No. 1, 1975, pp. 9–18.

[3]Waldman, C. H., "Theory of Non-Steady State Droplet Combustion," *Fifteenth Symposium (International) on Combustion*, Combustion Inst., Pittsburgh, PA, 1975, pp. 429–441.

[4]Nayagam, V., Haggard, J. B., Jr., Colantonio, R. O., Marchese, A. J., Dryer, F. L., Zhang, B. L., and Williams, F. A., "Microgravity *n*-Heptane Droplet Combustion in Oxygen–Helium Mixtures at Atmospheric Pressure," *AIAA Journal*, Vol. 36, No. 8, 1998, pp. 1369–1378.

[5]Fachini, F. F., "Combustión de Gotas Individuales y en Grupo," Doctoral Thesis, E.T.S. Ingenieros Aeronáuticos, Univ. Politécnica de Madrid, Madrid, Spain, July 1992.

[6]Fachini, F. F., and Liñán, A., "Transient Effects in Droplet Ignition Phenomenon," *Combustion and Flame*, Vol. 109, No. 3, 1997, pp. 303–313.

[7]Fachini, F. F., "Transient Effects in the Droplet Combustion Process in an Acoustically Perturbed High Temperature Environment," *Combustion Science and Technology*, Vol. 139, Nos. 1–6, 1998, pp. 173–190.

[8]Liñán, A., "The Asymptotic Structure of the Counterflow Diffusion Flame for Large Activation Energy," *Acta Astronautica*, Vol. 1, Nos. 7, 8, 1975, pp. 1007–1039.

[9]Sohrab, S. H., Liñán, A., and Williams, F. A., "Asymptotic Theory of Diffusion-Flame Extinction with Radiation Loss from the Flame Zone," *Combustion Science and Technology*, Vol. 27, Nos. 3, 4, 1982, pp. 143–154.

[10]Chao, B. H., Law, C. K., and T'ien, J. S., "Structure and Extinction of Diffusion Flames with Flame Radiation," *Twenty-Third Symposium (International) on Combustion*, Combustion Inst., Pittsburgh, PA, 1990, pp. 523–531.

[11]Saitoh, T., Yamazaki, K., and Viskanta, R., "Effect of Thermal Radiation on Transient Combustion of a Fuel Droplet," *Journal of Thermophysics and Heat Transfer*, Vol. 7, No. 1, 1993, pp. 94–100.

[12]Chang, K.-C., and Shieh, J.-S., "Theoretical Investigation of Transient Droplet Combustion by Considering Flame Radiation," *International Journal of Heat and Mass Transfer*, Vol. 38, No. 14, 1995, pp. 2611–2621.

[13]Marchese, A. J., and Dryer, F. L., "The Effect of Non-Luminous Thermal Radiation in Microgravity Droplet Combustion," *Combustion Science and Technology*, Vol. 124, Nos. 1–6, 1997, pp. 371–402.

[14]Liñán, A., and Williams, F. A., *Fundamentals Aspects of Combustion*, Oxiford Univ. Press, New York, 1993, pp. 145, 146.

[15]Law, C. K., "Asymptotic Theory for Ignition and Extinction in Droplet Burning," *Combustion and Flame*, Vol. 29, No. 1, 1975, pp. 89–98.

[16]Chung, C. H., and Law, C. K., "Structure and Extinction of Convective Diffusion Flames with General Lewis Numbers," *Combustion and Flame*, Vol. 52, No. 1, 1983, pp. 59–79.

[17]Liñán, A., and Rodrigues, M., "Droplet Vaporization, Ignition and Combustion," *Jornadas sobre Combustión en Motores Térmicos*, Univ. Politécnica de Madrid, Madrid, Spain, May 1985.

[18]Fachini, F. F., "The Effects of the Acoustics Field on Droplet Extinction Processes," *Combustion Science and Technology*, Vol. 120, Nos. 1–6, 1996, pp. 237–253.

[19]Fletcher, C. A. J., *Computational Techniques for Fluid Dynamics*, Vols. 1 and 2, 2nd ed., Springer–Verlag, Berlin, 1991.

[20]Cho, S. Y., Yetter, R. A., and Dryer, F. L., "Computer Model for One-Dimensional Mass and Energy Transport in and Around Chemically Reacting Particles, Including Complex Gas-Phase Chemistry, Multicomponent Molecular Diffusion, Surface Evaporation, and Heterogeneous Reaction," *Journal of Computational Physics*, Vol. 102, No. 1, 1992, pp. 160–179.

J. R. Bellan
Associate Editor